

# A multidimensional study of SIDIS charged Kaon beam spin asymmetry over a wide range of kinematics

Áron Kripkó, Stefan Diehl, Utsav Shrestha

Justus-Liebig University

*akripko@jlab.org*

December 13, 2022



Experimental Physics II

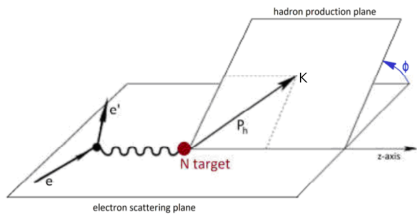
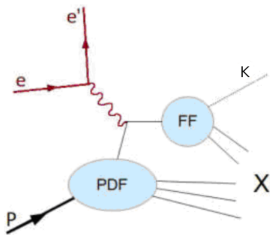


Jefferson Lab



# Physics motivation

- Kaon SIDIS:  $e^- p^+ \rightarrow e^- K^\pm X$
- polarised electron beam interacting with an un-polarised target:
- $d\sigma = d\sigma_0(1 + A_{UU}^{\cos\phi} \cos\phi + A_{UU}^{\cos 2\phi} \cos 2\phi + \lambda_e A_{LU}^{\sin\phi} \sin\phi)$
- $BSA = \frac{\sigma^+ - \sigma^-}{\sigma^+ + \sigma^-} = \frac{A_{LU}^{\sin\phi} \sin\phi}{1 + A_{UU}^{\cos\phi} \cos\phi + A_{UU}^{\cos 2\phi} \cos 2\phi}$



Process (left) and kinematics (right) of single kaon SIDIS

# Physics motivation

- Previous experiments (CLAS and HERMES) showed that kaon signals generally follow the pion signals, but they have larger values
- With these measurements the s-quark can be accessed, but due to the low statistics the uncertainties are large and the kinematic bins are wide
- The high statistics on an extended kinematic range, which is available with the new CLAS12, enables a fully differential analysis for the first time

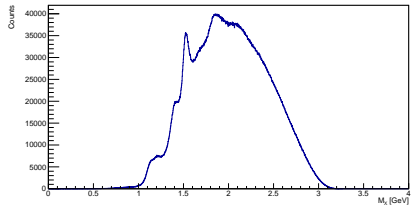
# Particle ID and dataset

- Eventbuilder particle ID
- Fiducial cuts - can be found in the common RG-A analysis note
- Electron and hadron PID refinements:
  - PCAL minimum energy deposition
  - ECAL sampling fraction cut
  - z-vertex position cut
  - Cut on vertex difference
  - $|\chi^2_{PID}| < 3$
- Use machine learning for Kaon ID
- QA cuts
- Topology: at least one good electron and at least one good Kaon
- Combine in- and outbending 10.6 GeV (2018) and inbending 10.2 GeV (2019) RG-A datasets:
  - 5032-5419
  - 5422-5666
  - 6616-6783

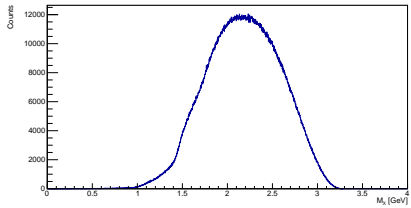
# Kinematic cuts

- $y < 0.75$  (minimal electron momentum of  $\sim 2.65$  GeV)
- $1.25 \text{ GeV} < p_K < 3 \text{ or } 5 \text{ GeV}$
- Only use forward detector for Kaons:
  - $5^\circ < \theta_K < 35^\circ$
  - $5^\circ < \theta_e < 35^\circ$
- To select the deep inelastic scattering region:
  - $W > 2 \text{ GeV}$
  - $Q^2 > 1 \text{ GeV}^2$
- To reject the kaons from the fragmentation region:
  - $x_F > 0$
  - $0.3 < z < 0.7$
- To reduce the contamination from exclusive processes:
  - $M_X > 1.6 \text{ GeV}$

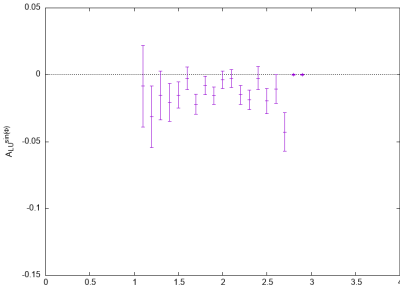
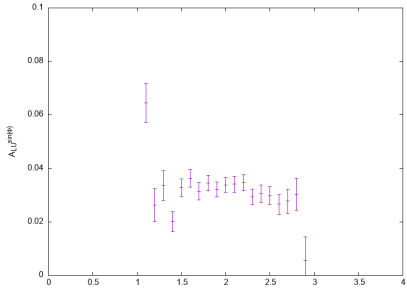
# Missing mass



$K^+$



$K^-$



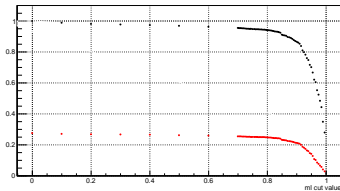
# Machine learning

- Reduce pion contamination in the kaon sample
- The main goal is not to identify pions and kaons but to get a clean kaon sample with reasonable statistics
- Use most of the available detector information available:
  - EventBuilder PID
  - Momentum and  $\beta$
  - Deposited energies in the 3 calorimeters
  - Calorimeter time information
  - Cluster moments and shower profiles
  - HTCC number of photoelectrons and time information
  - Energy depositions and time information in the 3 FTOF layers
- The results were cross-checked with another MC samples and with the RICH

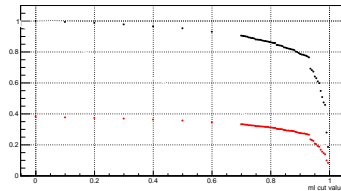
# Method used for training

- Toolkit: Root TMVA
- Deep neural network
  - 3 hidden layers with 128 neurons per layer
  - Fully connected
  - tanh activation function, linear for the last neuron
- Training
  - Crossentropy loss function
  - Xavier weight initialisation
  - Optimizer: ADAM
  - Batch size: 30
  - Learning rate:  $10^{-5}$
  - The input variables are normalised
  - The same amount of  $\pi$ -s and Kaons are used during the training

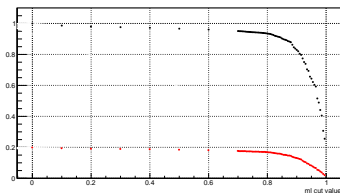
# Contamination and machine learning



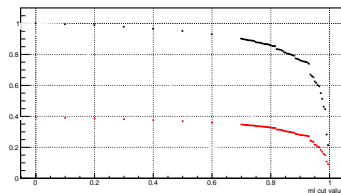
inbending,  $K^+$



inbending,  $K^-$



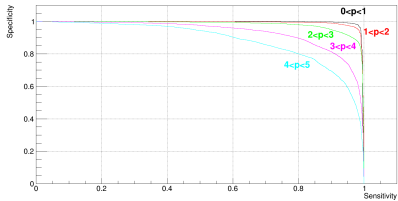
outbending,  $K^+$



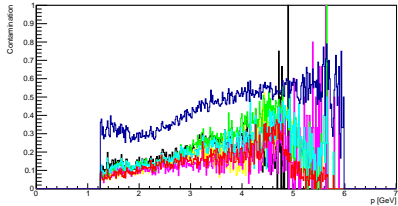
outbending,  $K^-$

Red - Contamination, Black - Efficiency

# Machine learning



ROC curves at different momenta ranges



Contamination obtained from simulated data

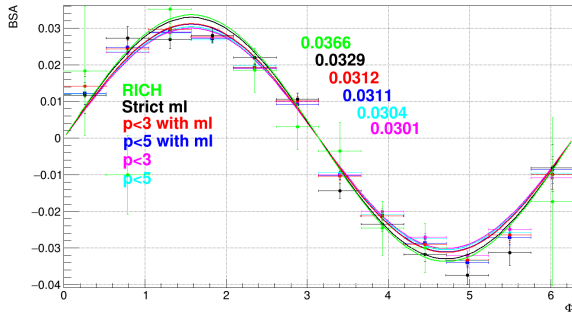
The resulting curve is red, when all variables are used during the training, yellow, when the EventBuilder PID and the  $\chi^2_{PID}$  is not used, green, when the FTOF is not used, blue, when the calorimeter is not used, purple, when the HTCC is not used and black, when only the momentum and  $\beta$  is used. In the contamination plot the results with the EventBuilder PID are plotted in dark blue for comparison.

# RICH-ML Correlation

RICH\EB	pion	Kaon	RICH\EB+ML	pion	Kaon
pion	104860	14454	pion	119253	2040
Kaon	2372	11514	Kaon	10001	4292

Correlation matrices of PID methods using kaons and pions in the RICH acceptance

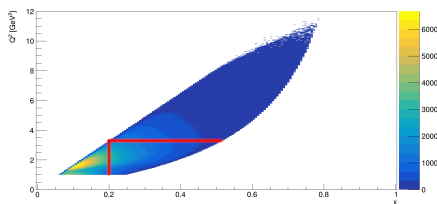
# Integrated asymmetry



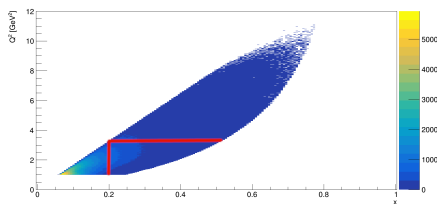
Integrated BSA values in bins of  $\Phi$  together with the fitted  $\sin \Phi$  functions for  $K^+$  using different PID methods: turquoise- $p < 5$  GeV, purple- $p < 3$  GeV, blue- $p < 5$  GeV and ml cut, red- $p < 3$  GeV and ml cut, black-strict(0.99) ml cut, green-RICH (in order of decreasing pion contamination)

# Multidimensional binning

- 3 bins on the  $x - Q^2$ -plane



$K^+$  with 3 bins



$K^-$  with 3 bins

Bin borders on the  $Q^2-x_B$ -plane

# Multidimensional binning

- 3 ( $K^+$ ) or 2 ( $K^-$ ) bins in  $P_T$  or  $x$

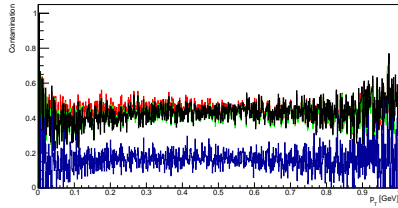
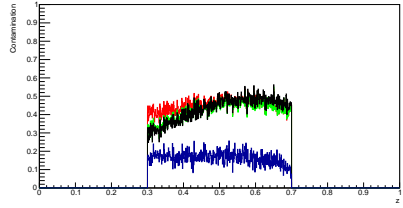
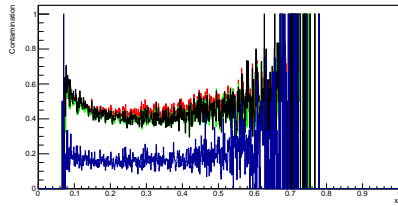
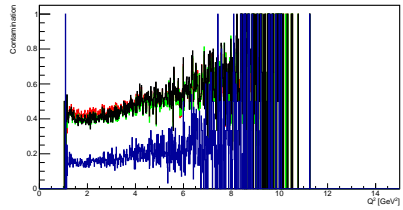
Bin number	$P_T$ bin	$x$ bin
1	$p_T < 0.33 \text{ GeV}$	$z < 0.34$
2	$0.33 \text{ GeV} < p_T < 0.66$	$0.34 < z < 0.52$
3	$p_T > 0.66 \text{ GeV}$	$z > 0.52$

Bin number	$P_T$ bin	$x$ bin
1	$p_T < 0.5 \text{ GeV}$	$z < 0.5$
2	$p_T > 0.5 \text{ GeV}$	$z > 0.5$

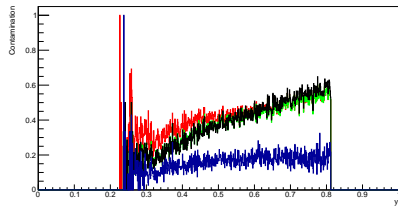
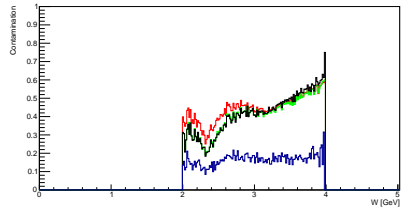
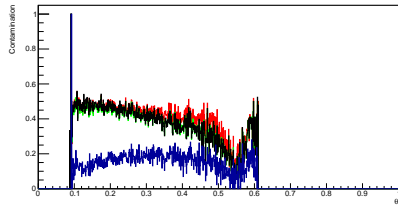
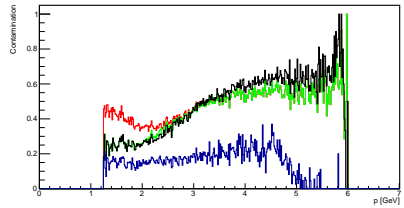
The binning for  $K^+$  (top) and for  $K^-$  (bottom)

- 10 bins in the last dimension -  $x$  or  $P_T$

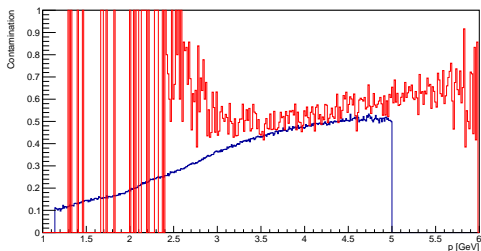
# Pion contamination



# Pion contamination



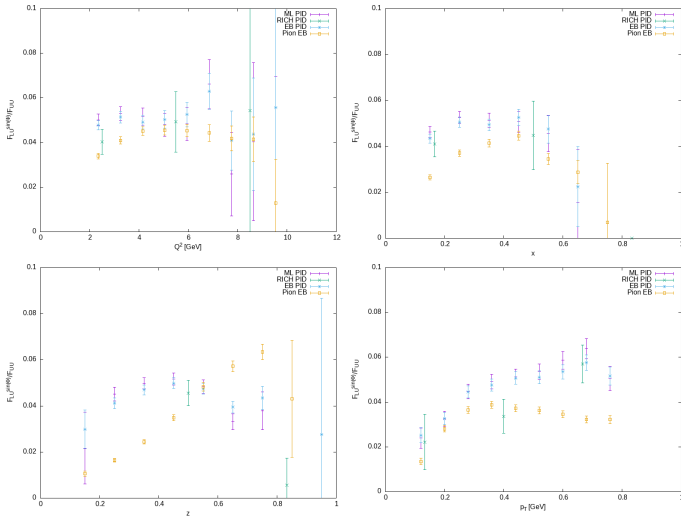
# Pion contamination, subtraction



Comparison of the kaon-pion contamination obtained from MC (blue) and from RICH (red) as a function of momentum using positive Eventbuilder kaons

- The pion contamination is too high - The pion asymmetries should be subtracted
- Contamination in a given bin:  
$$\frac{1}{N_{in}^{rec} + N_{out}^{rec} + N_{2019}^{rec}} \left( \frac{N_{inmc}^{mcm\pi}}{N_{inmc}^{rec}} (N_{in}^{rec} + N_{2019}^{rec}) + \frac{N_{outmc}^{mcm\pi}}{N_{outmc}^{rec}} N_{out}^{rec} \right)$$
- The asymmetry:  $\frac{AK_{meas} - CA_{meas}^{\pi}}{1-C}$

# Pion contamination, subtraction

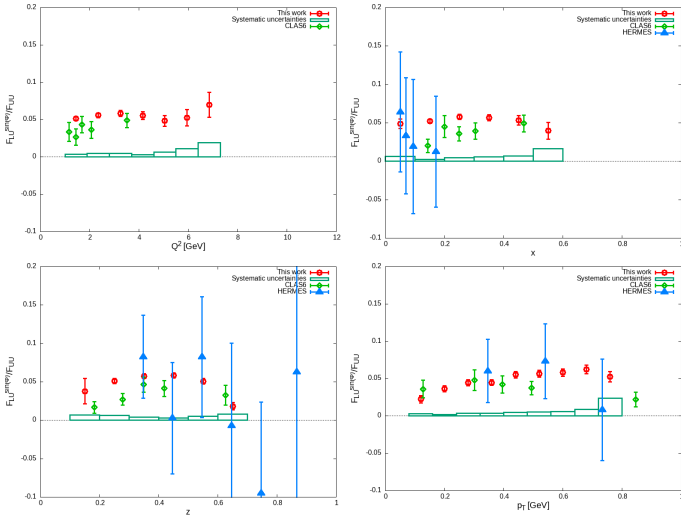


"Raw"  $F_{LU}^{\sin\phi}/F_{UU}$  as a function of  $Q^2$  (top left),  $x_B$  (top right),  $z$  (bottom left) and  $p_T$  (bottom right) for  $K^+$  with different PIDs compared with  $\pi^+$  results. The

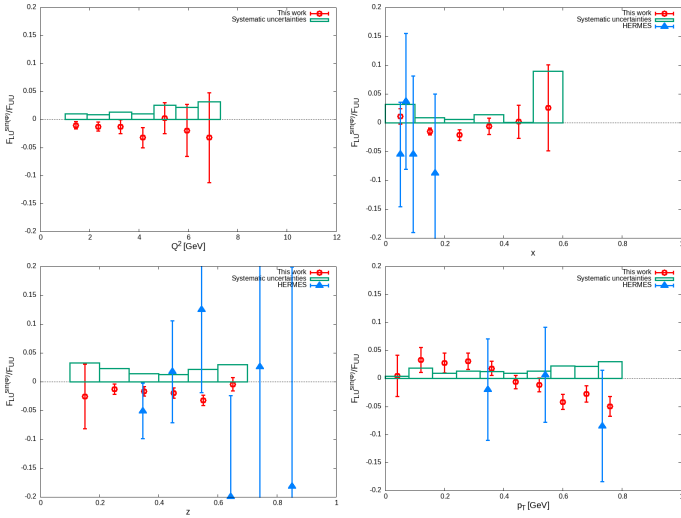
# Systematic uncertainties

- Most of the sources are the same as for the pion SIDIS note
- All uncertainties are determined for every kinematic bin
- Uncertainty of the beam polarization
- Effect of the fiducial cuts
- Contamination of the electron and Kaon samples
- Contamination of the SIDIS sample
- Acceptance effects
- Effect of the extraction method and higher order moments
- Bin migration and resolution effects
- Radiative effects
- Effects of the pion subtraction

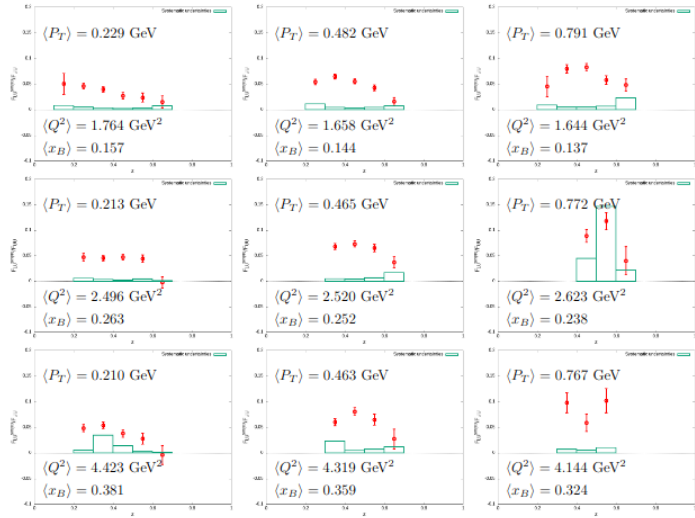
# Final 1D results - $K^+$



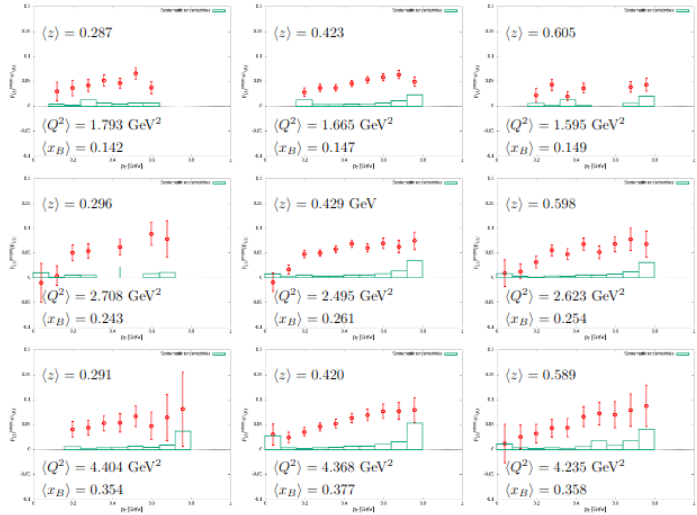
# Final 1D results - $K^-$



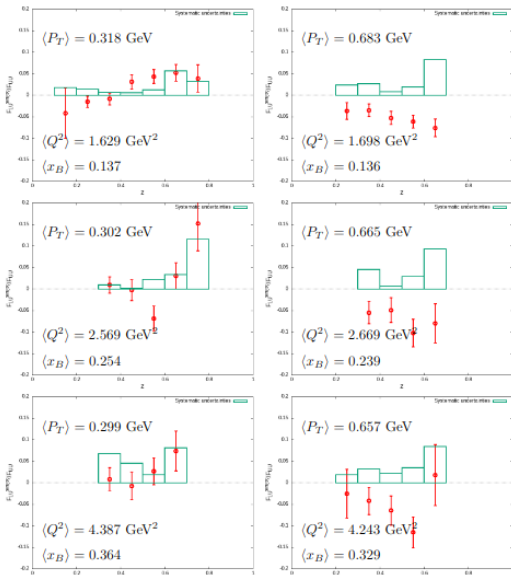
# Final 4D results - $K^+$



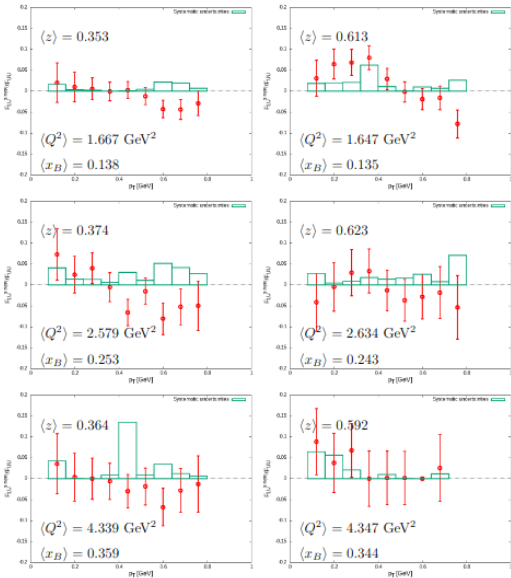
# Final 4D results - $K^+$



# Final 4D results - $K^-$



# Final 4D results - $K^-$

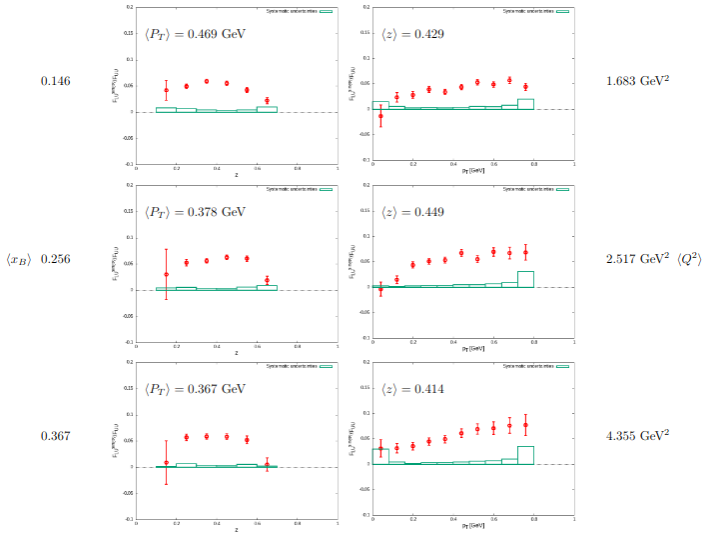


# Conclusion

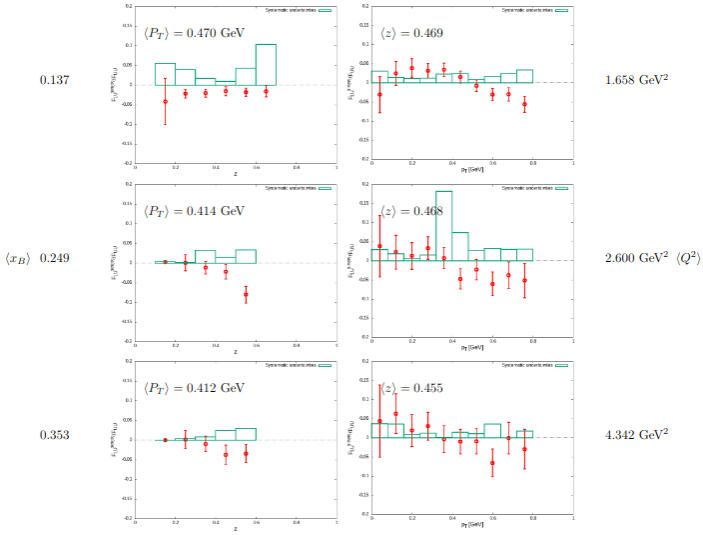
- The high statistics on an extended kinematic range, which is available with the new CLAS12, enables a fully differential analysis for the first time for charged kaons.
- The pion contamination is high, but it can be estimated and subtracted based on MC and ML.
- The contamination estimates should be confirmed. (RICH)
- The results follow the pion asymmetries in general, but they are higher. In some cases they have a slightly different behavior.
- The results are in agreement with the previous measurements.
- The analysis review is currently ongoing.

# Backup

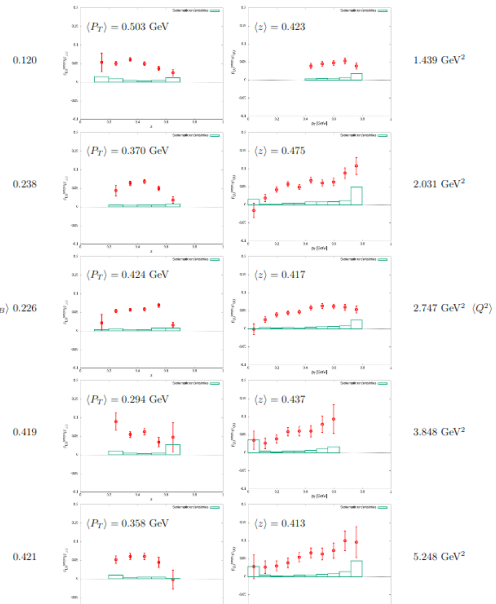
# Final 3D results - $K^+$



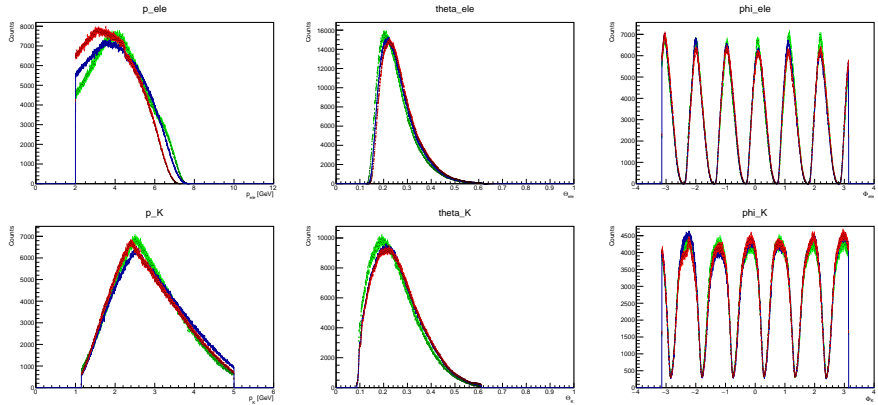
# Final 3D results - $K^-$



# Final 3D results - $K^+$

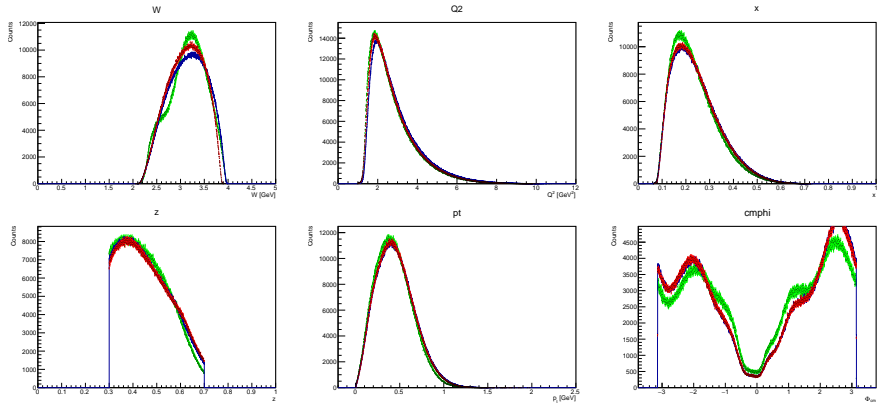


# Comparison with MC - K<sup>+</sup> inbedning



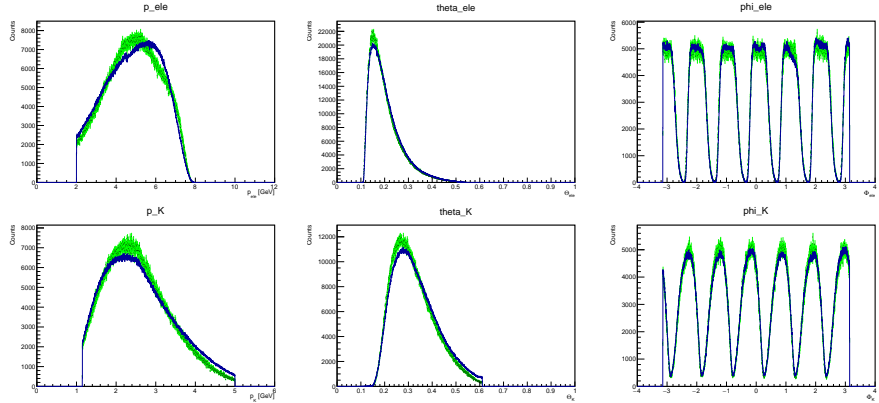
Comparison of the inbending simulated (green) and inbending experimental (blue-inbending, red-2019) distributions for the electron (up) and kaon (down) for the  $e^- K^+ X$  sample

# Comparison with MC - $K^+$ inbedning



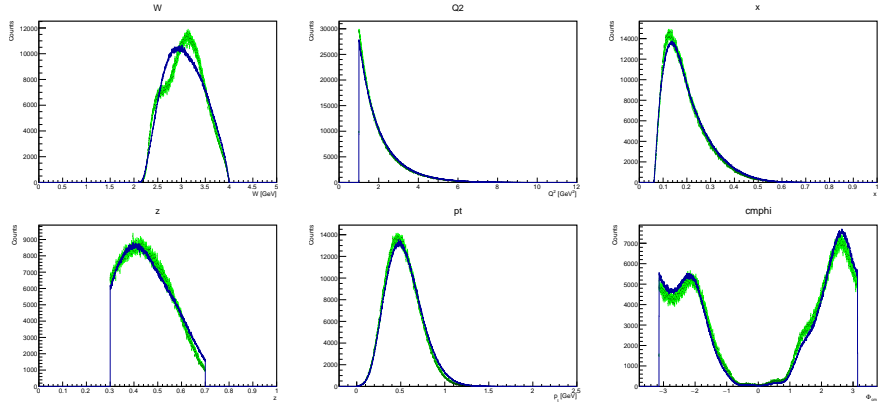
Comparison of the inbending simulated (green) and inbending experimental (blue-inbending, red-2019) kinematic distributions of  $W$ ,  $Q^2$ ,  $x_B$ ,  $z$ ,  $P_T$  and  $\phi$  for the  $e^- K^+ X$  sample

# Comparison with MC - $K^+$ outbedning



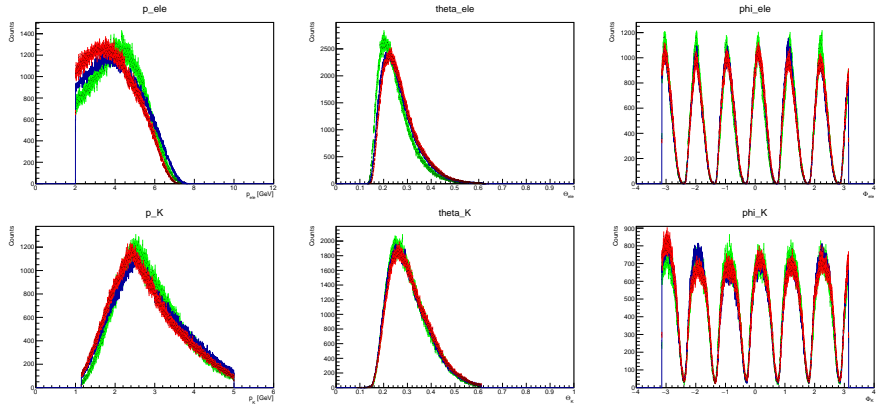
Comparison of the outbending simulated (green) and outbending experimental (blue) distributions for the electron (up) and kaon (down) for the  $e^- K^+ X$  sample

# Comparison with MC - $K^+$ outbedning



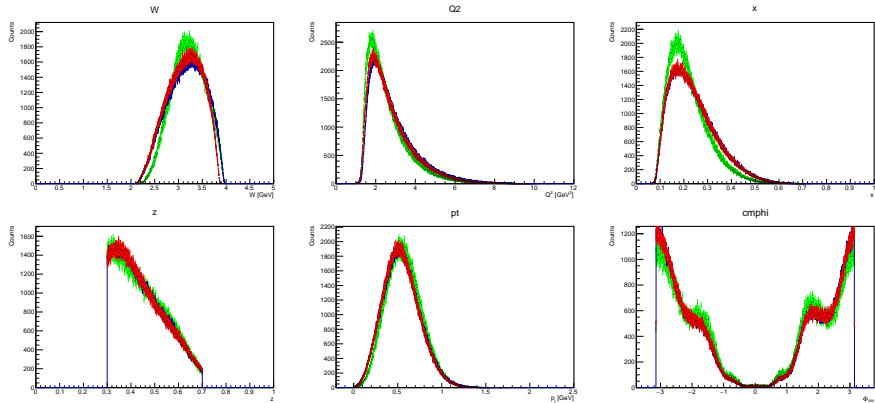
Comparison of the outbending simulated (green) and outbending experimental (blue) kinematic distributions of  $W$ ,  $Q^2$ ,  $x_B$ ,  $z$ ,  $P_T$  and  $\phi$  for the  $e^-K^+X$  sample

# Comparison with MC - $K^-$ inbedning



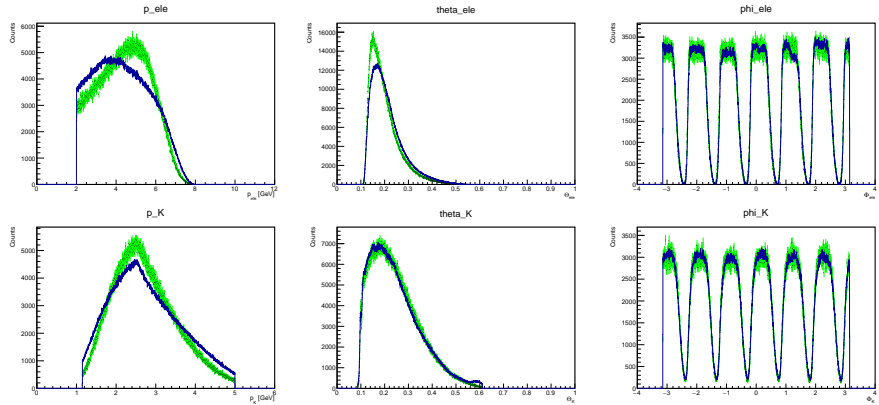
Comparison of the inbending simulated (green) and inbending experimental (blue-inbending, red-2019) distributions for the electron (up) and kaon (down) for the  $e^- K^- X$  sample

# Comparison with MC - $K^-$ inbedning



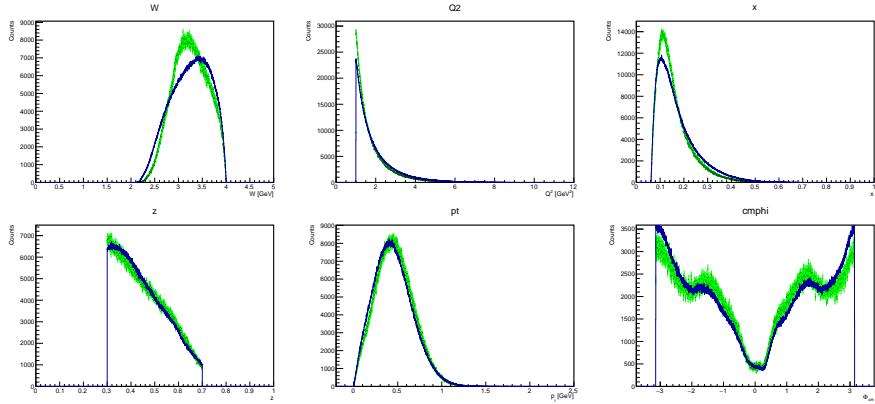
Comparison of the inbending simulated (green) and inbending experimental (blue-inbending, red-2019) kinematic distributions of  $W$ ,  $Q^2$ ,  $x_B$ ,  $z$ ,  $P_T$  and  $\phi$  for the  $e^- K^- X$  sample

# Comparison with MC - $K^-$ outbedning



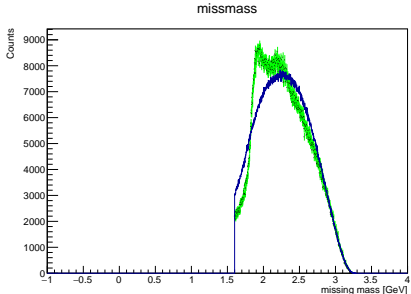
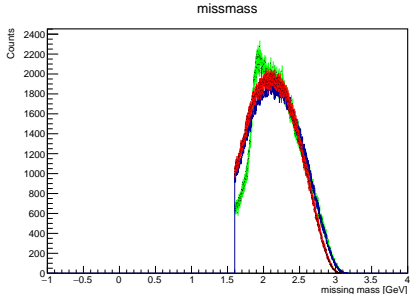
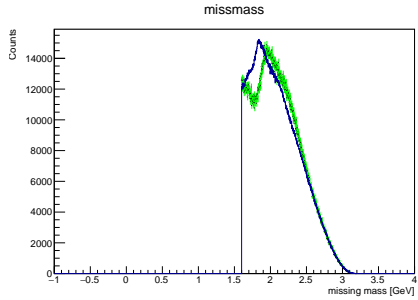
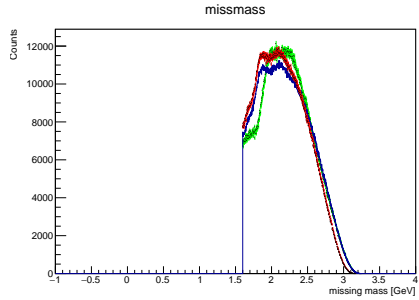
Comparison of the outbending simulated (green) and outbending experimental (blue) distributions for the electron (up) and kaon (down) for the  $e^- K^- X$  sample

# Comparison with MC - $K^-$ outbedning

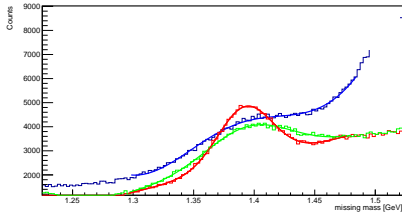
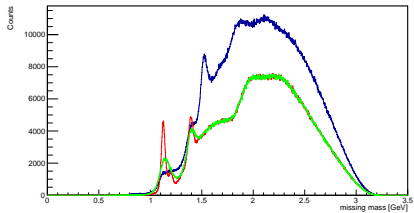


Comparison of the outbending simulated (green) and outbending experimental (blue) kinematic distributions of  $W$ ,  $Q^2$ ,  $x_B$ ,  $z$ ,  $P_T$  and  $\phi$  for the  $e^- K^- X$  sample

# Comparison with MC - K<sup>+</sup> inbedning

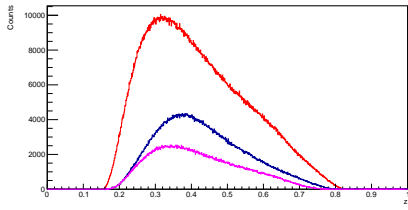
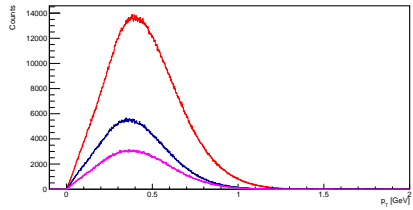


# MC Smearing



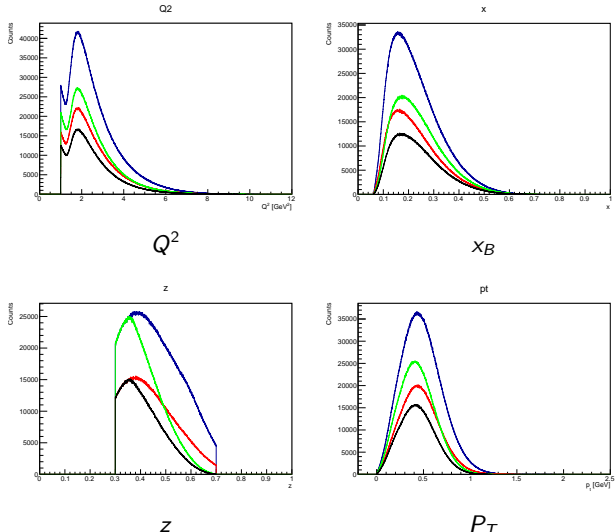
Comparison of the simulated with (green) and without the smearing (red) and experimental (blue) missing mass distributions in the inbending setting for the  $e^-K^+X$  sample on the whole missing mass range (left) and near the peak at 1.4 GeV (right)

# Multidimensional binning - $K^-$



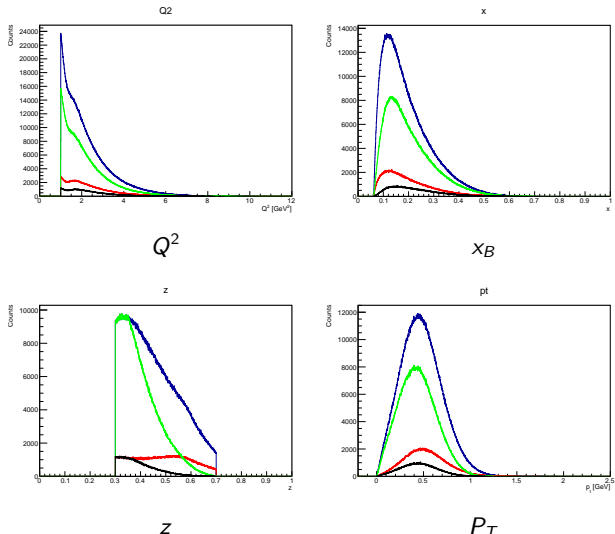
$P_T$  (left) and  $z$  (right) distributions in different  $Q^2-x_B$  bins (red - bin 1, blue - bin 2, purple - bin 3) for the  $e^- K^- X$  dataset with  $p_K < 5$  GeV cut

# Kinematics - K<sup>+</sup>



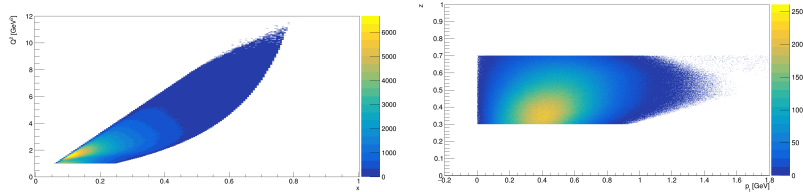
blue:  $p_K < 5 \text{ GeV}$ , red:  $p_K < 5 \text{ GeV}$  with  $ml$ , green:  $p_K < 3 \text{ GeV}$ , black:  $p_K < 3 \text{ GeV}$  with  $ml$ , grey:  $p_K < 3 \text{ GeV}$  with both  $ml$  and  $ml$

# Kinematics - $K^-$

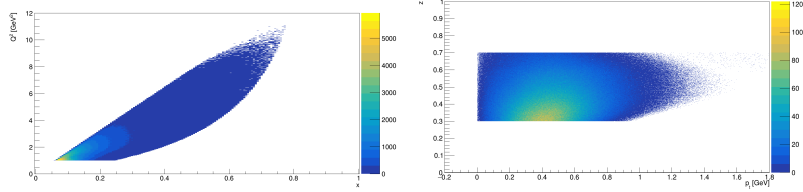


blue:  $p_K < 5 \text{ GeV}$ , red:  $p_K < 5 \text{ GeV}$  with ml, green:  $p_K < 3 \text{ GeV}$ , black:  $p_K < 3 \text{ GeV}$  with ml, grey:  $p_K < 3 \text{ GeV}$

# Correlation

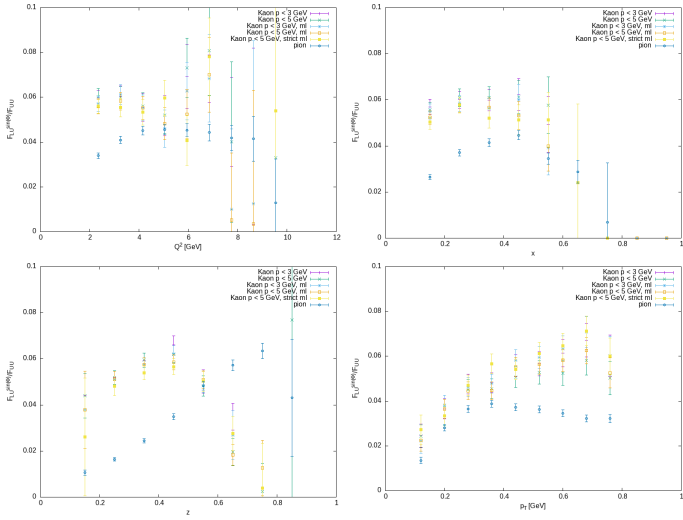


The correlations of  $Q^2-x_B$  (left) and  $P_T-z$  (right) for the  $e^-K^+X$  sample with  $p_K < 5$  GeV cut

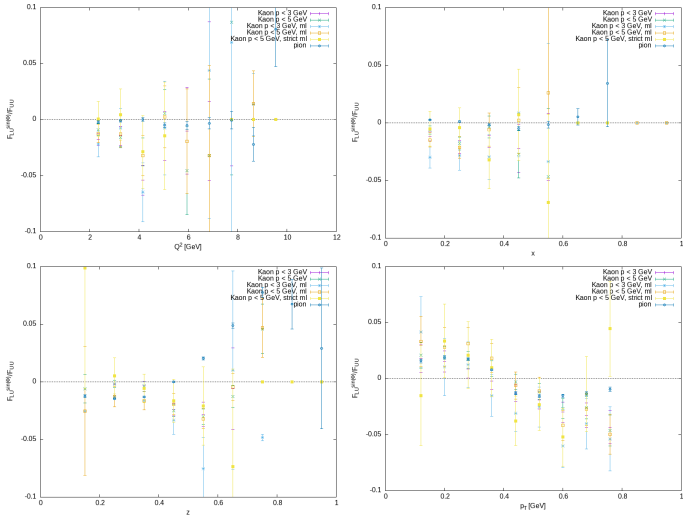


The correlations of  $Q^2-x_B$  (left) and  $P_T-z$  (right) for the  $e^-K^-X$  sample with  $p_K < 5$  GeV cut

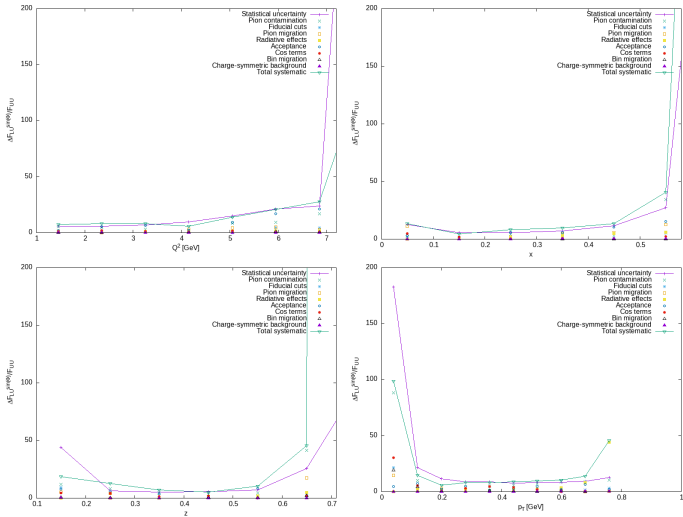
# After pion subtraction - $K^+$



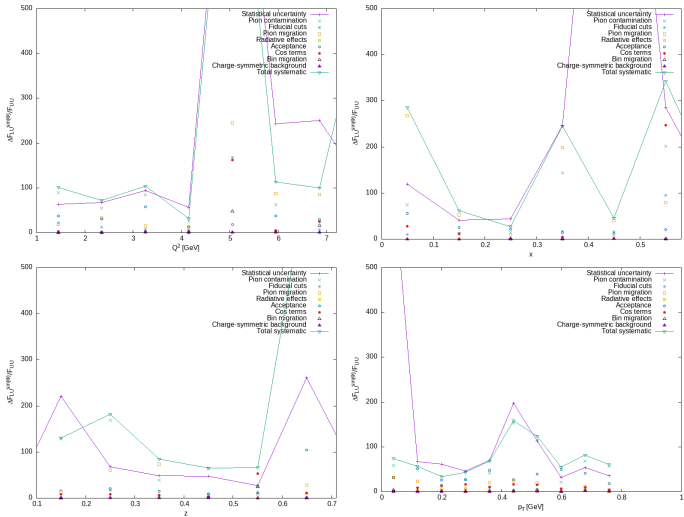
# After pion subtraction - $K^-$



# Systematic uncertainties - $K^+$

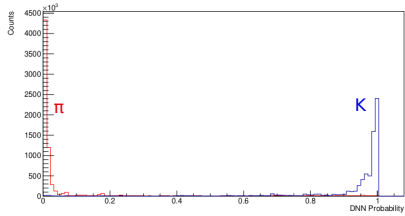


# Systematic uncertainties - $K^-$

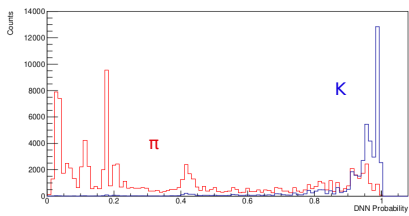


# Return value

- The output from the neural network is a value between 0 and 1
- Red: mc  $\pi$ -s
- Blue: mc Kaons
- Cuts: 0.96 (standard) or 0.99 (strict)

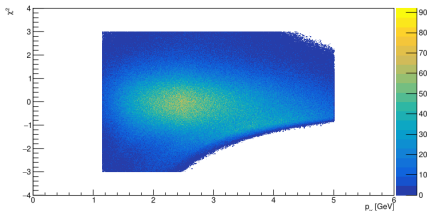


Whole  $p$  range

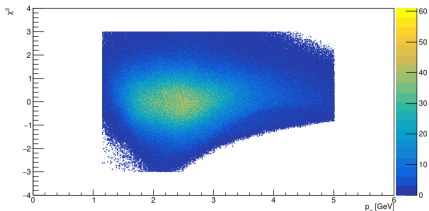


$p > 3$  GeV

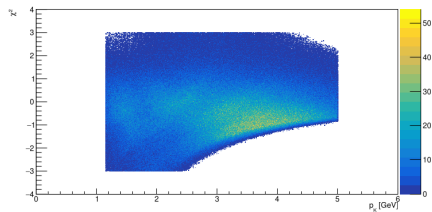
# PID $\chi^2$



Without machine learning



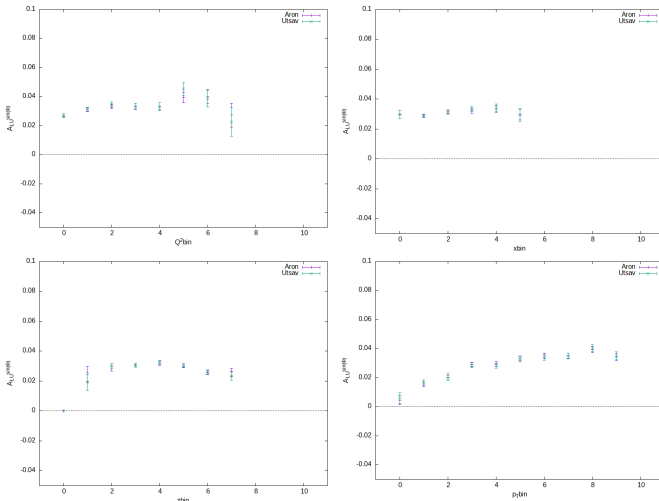
With machine learning



Difference - removed particles

# Cross-checks - Utsav Shrestha

- Almost complete agreement in the number of particles, their kinematics,  $N^\pm$  and BSA
- Minor  $A_{LU}$  differences - in bins which are removed from the results

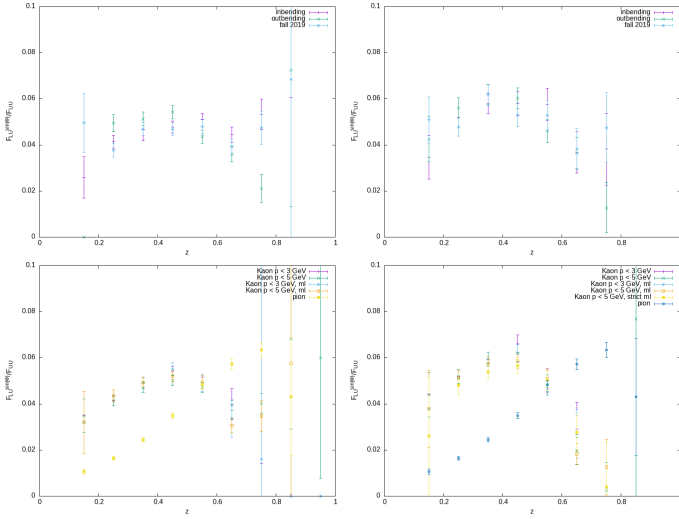


# Multidimensional binning - Average uncertainty

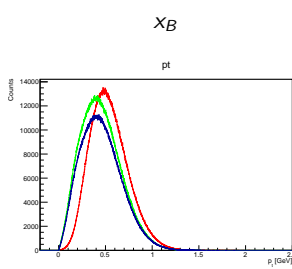
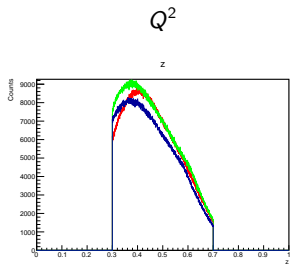
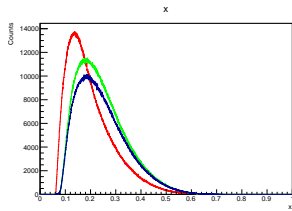
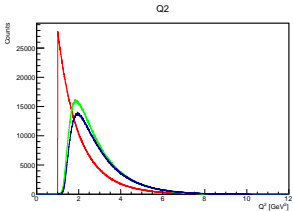
Source	Relative uncertainty		Absolute uncertainty	
	$K^+$	$K^-$	$K^+$	$K^-$
Statistical uncertainty	28.8%	123.7%	0.012	0.023
Pion contamination	11.5%	79.9%	0.005	0.015
Beam polarization	2.8%	3.2%	0.001	0.001
Fiducial cuts	8.5%	29.3%	0.003	0.006
Pion bin migration	5.3%	50.3%	0.002	0.009
Radiative effects	3.3%	1.1%	0.001	0.0002
Acceptance	3.5%	31.4%	0.001	0.006
Cos terms	5.4%	32%	0.002	0.006
Bin migration	1.8%	3.2%	0.001	0.001
Phi bin migration	1%	1%	0.0004	0.0001
Charge-symmetric bg.	0.2%	0.5%	0.0001	0.0002
Accidentals	1%	1%	0.0004	0.0001
Total systematic uncert.	21.6%	89.9%	0.009	0.017

Relative and absolute uncertainty from the different sources averaged over all bins ↗

# Before (left) and after (right) subtraction



# Comparison of different datasets - K<sup>+</sup>

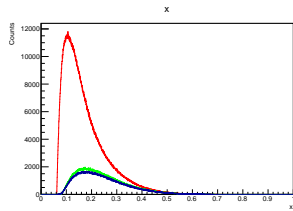
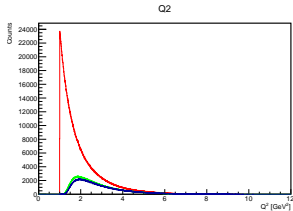


z

$P_T$

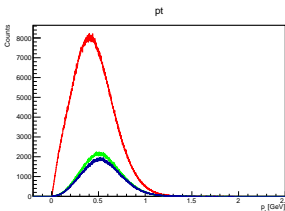
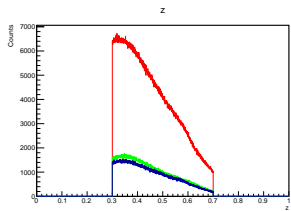
blue-inbending fall 2018, red-outbending fall 2018, green-inbending spring 2019

# Comparison of different datasets - $K^-$



$Q^2$

$x_B$

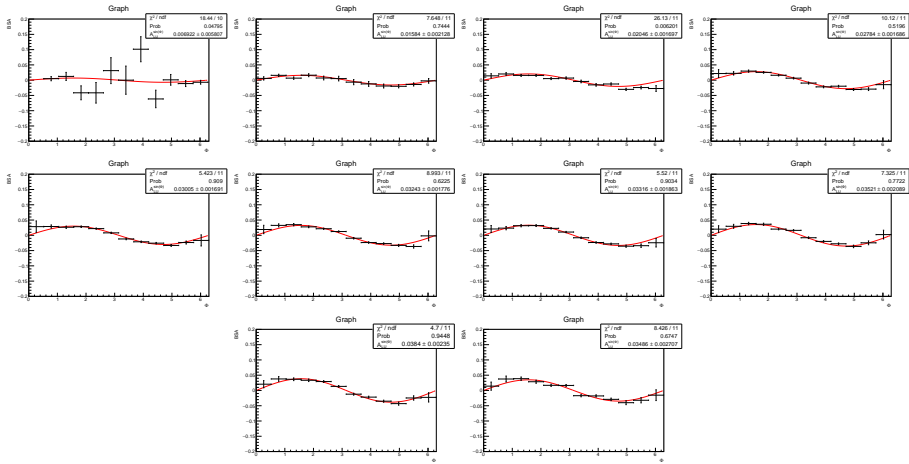


z

$P_T$

blue-inbending fall 2018, red-outbending fall 2018, green-inbending spring 2019

# BSA fit examples



BSA in  $P_T$  bins in increasing order from top left to bottom right for the  $e^- K^+ X$  dataset with  $p_K < 5$  GeV cut